

ACCEPTED MANUSCRIPT

Interfacial-engineering enhanced performance and stability of ZnO nanowire-based perovskite solar cells

To cite this article before publication: Junlu Sun *et al* 2021 *Nanotechnology* in press <https://doi.org/10.1088/1361-6528/abdbeb>

Manuscript version: Accepted Manuscript

Accepted Manuscript is “the version of the article accepted for publication including all changes made as a result of the peer review process, and which may also include the addition to the article by IOP Publishing of a header, an article ID, a cover sheet and/or an ‘Accepted Manuscript’ watermark, but excluding any other editing, typesetting or other changes made by IOP Publishing and/or its licensors”

This Accepted Manuscript is © 2020 IOP Publishing Ltd.

During the embargo period (the 12 month period from the publication of the Version of Record of this article), the Accepted Manuscript is fully protected by copyright and cannot be reused or reposted elsewhere.

As the Version of Record of this article is going to be / has been published on a subscription basis, this Accepted Manuscript is available for reuse under a CC BY-NC-ND 3.0 licence after the 12 month embargo period.

After the embargo period, everyone is permitted to use copy and redistribute this article for non-commercial purposes only, provided that they adhere to all the terms of the licence <https://creativecommons.org/licenses/by-nc-nd/3.0>

Although reasonable endeavours have been taken to obtain all necessary permissions from third parties to include their copyrighted content within this article, their full citation and copyright line may not be present in this Accepted Manuscript version. Before using any content from this article, please refer to the Version of Record on IOPscience once published for full citation and copyright details, as permissions will likely be required. All third party content is fully copyright protected, unless specifically stated otherwise in the figure caption in the Version of Record.

View the [article online](#) for updates and enhancements.

Interfacial-engineering enhanced performance and stability of ZnO nanowire-based perovskite solar cells

Junlu Sun^{1,2†}, Nengxu Li^{4†}, Lin Dong^{1*}, Xiuxiu Niu⁴, Mengqi Zhao², Ziqi Xu⁴, Huanping Zhou^{4*}, Chongxin Shan¹, Caofeng Pan^{2,3*}

¹ Henan Key Laboratory of Diamond Optoelectronic Materials and Devices, School of Physics and Microelectronics, Zhengzhou University, 450001, PR China

² CAS Center for Excellence in Nanoscience, Beijing Key Laboratory of Micro-nano Energy and Sensor, Beijing Institute of Nanoenergy and Nanosystems, Chinese Academy of Sciences, Beijing 100083, PR China

³ School of Nanoscience and Technology, University of Chinese Academy of Sciences, Beijing 100049, PR China

⁴ Department of Materials Science and Engineering, Peking University, Beijing 100871, PR China

[†] These authors contributed equally to this work.

E-mail: ldong@zzu.edu.cn, happy_zhou@pku.edu.cn and cfpan@binn.cas.cn

Received xxxxxx

Accepted for publication xxxxxx

Published xxxxxx

Abstract

Perovskite solar cells (PSCs) have attracted extensive attention due to their convenient fabrication and excellent photoelectric characteristics. The highest power conversion efficiency (PCE) of over 25 % has been realized. However, ZnO as electron transport layer (ETL) based PSCs exhibit inferior PCE and stability because of the mismatched energy-band and undesirable interfacial recombination. Here, we introduce a thin layer of SnO₂ nanocrystals to construct an interfacial engineering with gradient energy band and interfacial passivation via a facile wet chemical process at a low temperature. The best PCE obtained in this study reaches 18.36 %, and the stability is substantially improved and maintains a PCE of almost 100 % over 500 h. The low-temperature fabrication process facilitates the future application of ZnO/SnO₂-based PSCs in flexible and stretchable electronics.

Keywords: perovskite solar cell, gradient energy band, interfacial passivation, stability

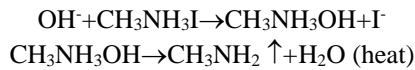
1. Introduction

Perovskite materials have been widely utilized for a variety of optoelectronic devices, including light-emitting diodes [1-5], lasers [6-8], photodetectors [9-11], and solar cells [12-16], due to their excellent photoelectric characteristics such as high absorption coefficients and long exciton diffusion lengths [17,18]. The highest PCE of perovskite solar cells has been reported over 25 % [16,19], which make it possible to be used in flexible and stretchable electronics [20,22]. ZnO with a high electron mobility [23], good crystallinity, and similar energy

band level [24-26], could be an ideal electron transport layer in PSCs. The ZnO nanowires could be obtained through various methods (e.g. low-temperature H₂O oxidation [27,28], room-temperature sputter [29], atomic layer deposition [30], hydrothermal method [16]), in which the hydrothermal method provides a favorable way to fabricate high-performance and flexible PSCs.

However, ZnO nanowire-based PSCs usually demonstrate inferior PCEs and stability, mainly due to their substantial surface state-mediated recombination via recombination centers in the defects and dangling bonds introduced during

the fabrication process, especially when exposed to the air [31,32]. The poor stability of ZnO nanowire-based PSCs is another serious issue for the deprotonation reaction of methylammonium cations at the interface between ZnO and perovskite [33]. The chemical products, such as alkaline and hydroxyl groups at the surface of wet chemical synthesized ZnO, could then deteriorate the $\text{CH}_3\text{NH}_3\text{PbI}_3$ (MAPbI₃) via the following reaction process:



Some ZnO/SnO₂ nanocomposites as ETLs have been provided to improve the performance of perovskite solar cells, for example, core-shell ZnO@SnO₂ nanoparticles [34], ZnO/SnO₂ bilayers nanoparticles [35], and SnO₂ film on the ZnO dense layer [36]. The ZnO nanowires possess high electron mobility and easy-fabricating through hydrothermal method. What's more, the piezoelectricity of ZnO nanowires could also be utilized to improve the performance of PSCs.

Here, we construct an interfacial engineering with a gradient energy band interfacial passivation through comprising a ZnO/SnO₂/perovskite structure. The layer of SnO₂ nanocrystal is introduced between the ZnO ETL and perovskite active layer to build matched energy-band and prevent the deprotonation reaction at the interface of the ZnO

diagram. The position of the conduction band minimum (CBM) of the ZnO nanowire and SnO₂ can be derived from their work function (W_s), valence band maximum (VBM), and energy bandgap width (E_g) according to Equation

$$\text{CBM} = W_s + \text{VBM} - E_g$$

where W_s , VBM, and E_g can be determined by the ultraviolet photoelectron spectroscopy (UPS) cutoff edge, UPS and UV-Vis absorption spectroscopy, respectively, as shown in Figure 2a-c.

The profoundly mismatched CBM of ZnO (4.50 eV) and MAPbI₃ (3.93 eV) significantly restricts the photovoltaic output for ZnO-based PSCs with large low energy losses (E_{loss}). The SnO₂ nanocrystals with an elevated CBM (4.23 eV) offer a more aligned energy level with the MAPbI₃. As a consequence, the energy level gradient in the ZnO/SnO₂ ETL and MAPbI₃ layer establishes a favorable matching of the cascade energy band, which facilitates effective extraction of photogenerated electrons from the perovskite layer to the ITO electrode. The fabrication process is detailed in Figure S1 in the Supporting Information.

The typical structure of the PSCs with a ZnO/SnO₂ energy level gradient engineered with an ETL is demonstrated in Figure 3a. The ZnO nanowires (NWs) with diameters of approximately 60 nm were grown uniformly atop the ITO

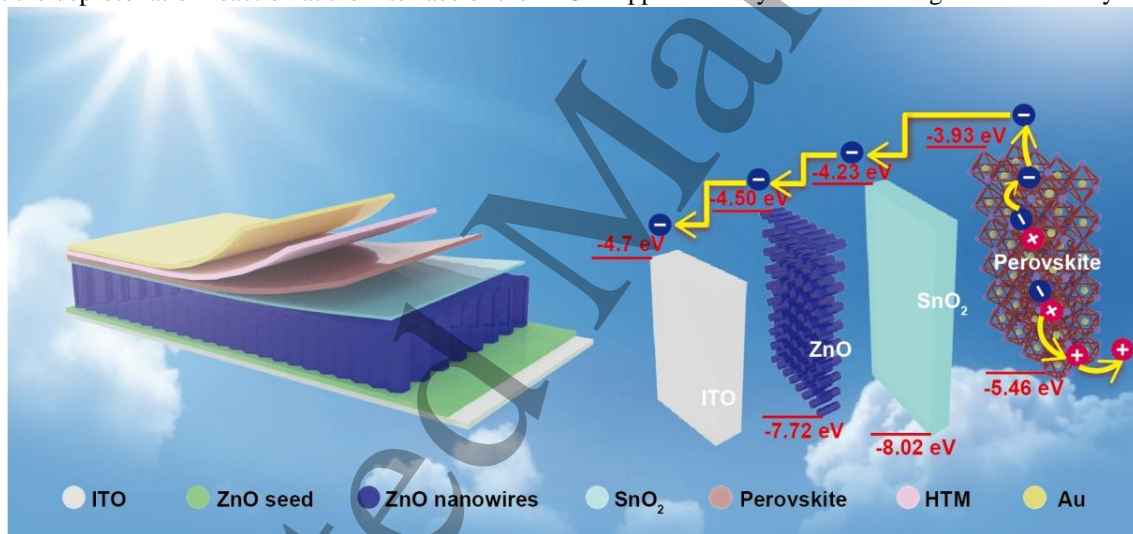


Figure.1 Diagram of ZnO-based perovskite solar cells with interfacial engineering.

nanowires and perovskite. A tremendous enhancement of 32.7 % was realized in their average PCEs, and the best PCE obtained in this study reaches 18.36 %. Furthermore, the stability of these PSCs with an interfacial engineering is greatly improved in comparison with the ZnO nanowire-based PSCs. The interfacial engineering not only enhance performance but also improve the stability of ZnO nanowire-based perovskite solar cells.

2. Results and Discussion

The PSCs with an interfacial engineering comprise an architecture of ITO/ZnO/SnO₂/MAPbI₃/Spiro-OMeTAD/Au, as illustrated in Figure 1 and the corresponding energy band

(Figure 3b). Then, a layer of SnO₂ nanocrystals with a thickness of 80 nm was deposited onto the ZnO NWs Figure 3c. The cross-section SEM image of the ZnO/SnO₂ structure shown in Figure S3a confirms that the ZnO NWs were completely covered and passivated by the SnO₂ nanocrystals. The composition of the ZnO/SnO₂ layer was further identified by the energy dispersive spectrum (EDS), comprising of O, Zn, and Sn, which was also indicated by the EDS mapping images shown in Figure S3c-e.

The performances of the PSCs with and without interfacial engineering are shown in Figure 4. The J-V curves measured with a 50 ms scanning delay under AM 1.5 solar illuminations

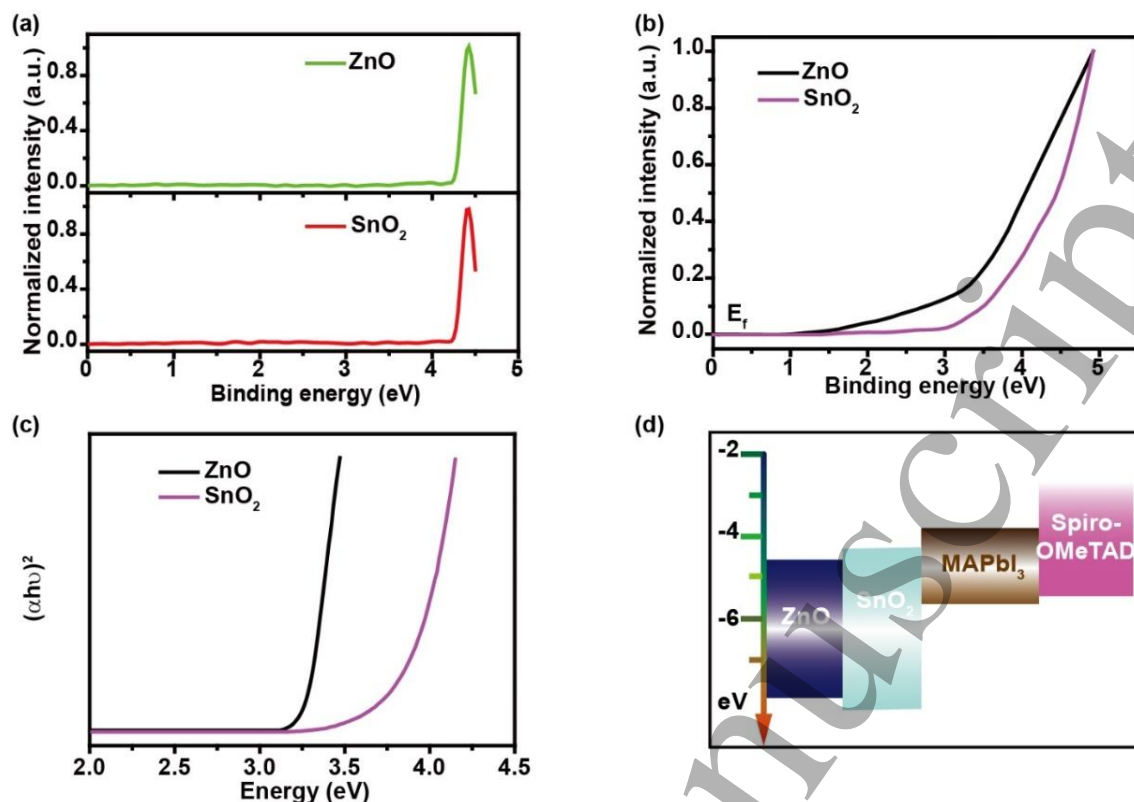


Figure.2 Energy band features of ZnO NWs and SnO₂ nanocrystals. (a) Ultraviolet photoelectron spectroscopy cut-off edges of ZnO (black) and SnO₂ (purple). (b) Valence band spectra of ZnO (black) and SnO₂ (purple) derived from UPS measurements. (c) The bandgap values of ZnO (black) and SnO₂ (purple) from the relationship of $(\alpha h\nu)^2$ versus photon energy. (d) Energy band alignment of the energy level gradient in the ETL perovskite solar cell

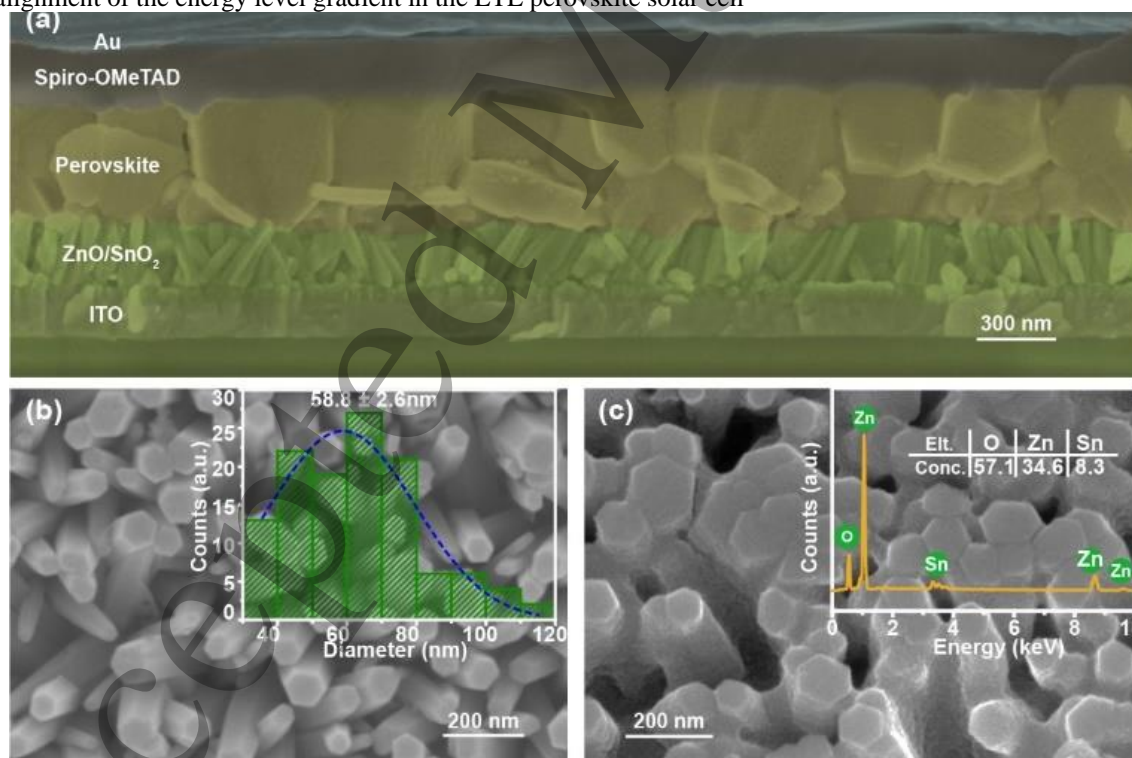


Figure.3 (a) Cross-section SEM image of ZnO/SnO₂-based perovskite solar cells. SEM image of ZnO NWs (b) before and (c) after being covered with SnO₂ nanocrystals. Inset: energy dispersive X-ray spectra of the ZnO/SnO₂ ETLs with an energy band gradient.

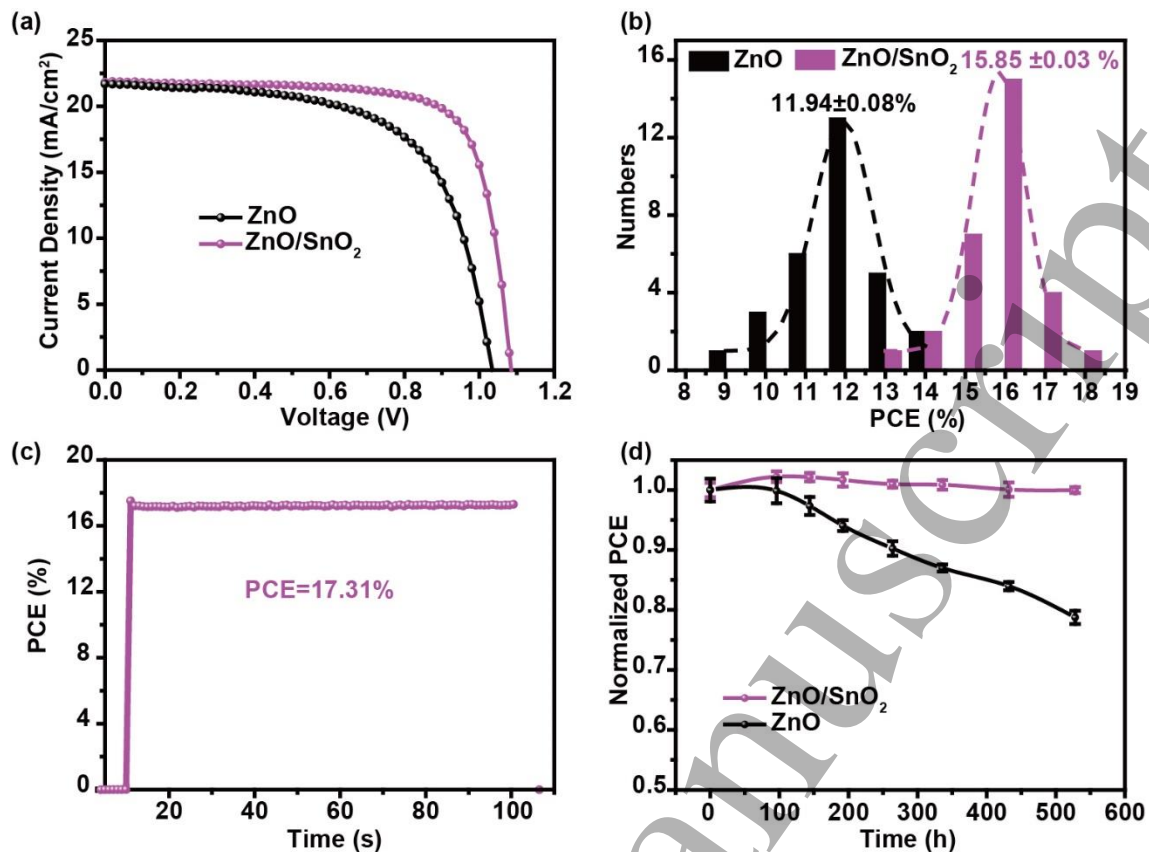


Figure 4 (a) J-V characterizes the ZnO nanowire-based PSC and ZnO/SnO₂-based PSC under AM 1.5 solar illumination at ambient conditions. (b) Statistical analysis of PCE results of ZnO nanowire-based PSCs with a mean value of $11.94 \pm 0.08\%$; the ZnO/SnO₂-based PSCs had a mean value of $15.85 \pm 0.03\%$ and a maximum value of 18.36%. (c) The time-dependent stabilized power output of the ZnO/SnO₂ ETL-based PSCs with an energy level gradient measured at the maximum power point. (d) Normalized efficiency of ZnO nanowire-based PSCs and ZnO/SnO₂-based PSCs in N₂-filled glove boxes.

under ambient conditions are presented in Figure 4a. The V_{oc} , J_{sc} and FF of the ZnO/SnO₂ ETL PSC with an interfacial engineering were 1.09 V, 22.16 mA/cm² and 76.12 %, respectively, with a highest PCE obtained in this study of 18.36 %. The champion device was measured under different scan directions, which showed little influence on the performance (Figure S4). The black line in Figure 4a presents the optimized performance of the ZnO nanowire-based PSC, of which the PCE, V_{oc} , J_{sc} , and FF were 14.33 %, 1.04 V, 21.26 mA/cm², and 65.14 %, respectively. To verify the reliability of the performance enhancement with the introduction of the interfacial engineering, the PCE statistics for all the ZnO/SnO₂-based PSCs in one batch (30 cells) are illustrated in Figure 4b as the purple histogram ranging from 13.5 % to 18.3 %, where the most populated efficiency was 15.85 %. The black histogram in Figure 4b shows the PCE statistics of the ZnO-based PSCs (30 cells) ranging from 9 % to 14.4 % with a numerical average value of 11.94 %. The statistical analysis of the V_{oc} , J_{sc} , FF, and PCE are also presented in Figure S5 to determine the average performance of PSCs with an interfacial engineering compared PSCs without an interfacial engineering. An enhancement in the

PCE of over 30 % was obtained by introducing a SnO₂ nanocrystal as interfacial engineering between the ZnO NWs and perovskite. The time-dependent power output of the champion device was evaluated by tracking the efficiency at the maximum power point conditions. The PSCs engineered with a gradient in the energy band exhibited a highly stable power output, which may eliminate the variation of the efficiency due to the light soaking effects [37]. The long-term thermal stability of the unencapsulated PSCs with and without interfacial engineering was monitored by curing the cells at 40 °C in a glove box for 536 h, as shown in Figure 4d. The PCEs of the ZnO/SnO₂-based PSCs maintained almost 100 % of their original value (shown in Figure 4d by the purple line), while that of the ZnO nanowire-based PSCs decreased by approximately 25 %. This evidence supports the suppression of the deprotonation reaction between the ZnO NWs and perovskites after the introduction of the SnO₂ nanocrystals as the interfacial passivation engineering. Consequently, the thermal stability of the ZnO nanowire-based PSCs was profoundly enhanced through the interfacial gradient energy band engineering and interfacial passivation engineering.

To explore the internal mechanism of the performance improvement induced by ETL structure with an energy band gradient, steady-state photoluminescence (PL), time-resolved photoluminescence (TRPL), external quantum efficiency (EQE) and electrochemical impedance spectroscopy (EIS) measurements were carried out to study the interfacial effects

resistance (R_{rec}) can be derived from the low-frequency range semicircle and the corresponding equivalent circuit (Figure S6). Clearly, the ZnO/SnO₂-based PSC had a larger R_{rec} value (approximately 75 K Ω) than the ZnO nanowire-based cell (approximately 30 K Ω). The larger R_{rec} could effectively suppress the charge recombination, enhancing the PCE of

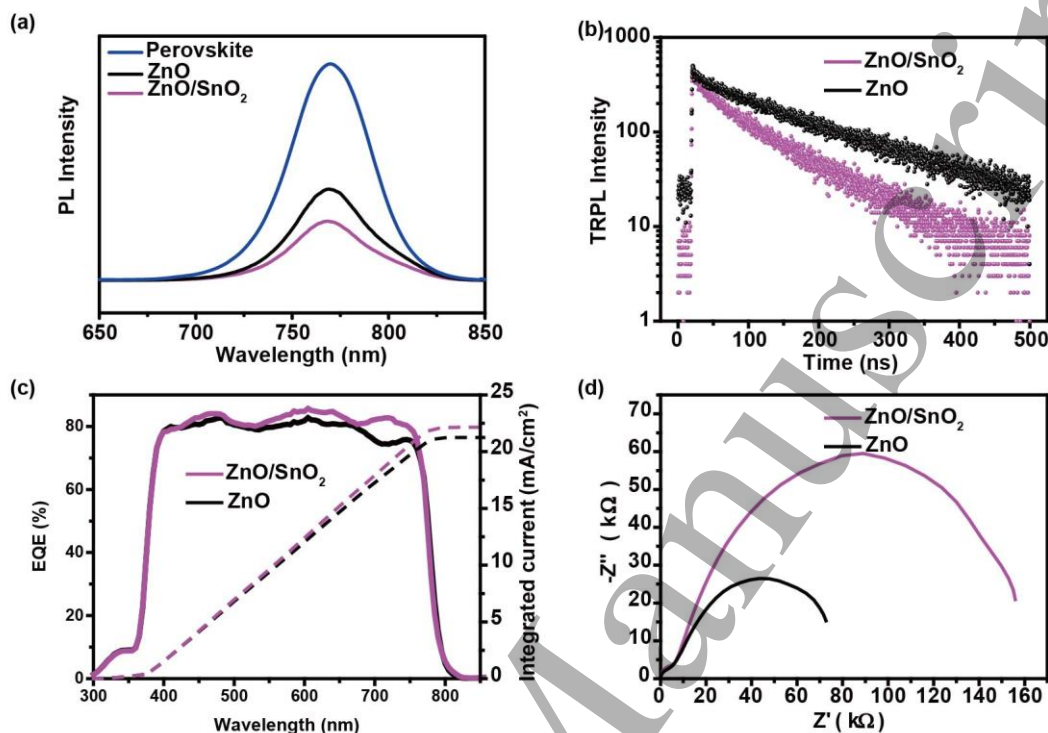


Figure.5 (a) Room temperature photoluminescence (PL) spectra of the perovskite-coated ZnO NWs and SnO₂ nanocrystals covering the ZnO NWs. (b) Time-resolved photoluminescence (TRPL) spectra of the perovskite-coated ZnO NWs and SnO₂ nanocrystals covering ZnO NWs. (c) The external quantum efficiency (EQE) spectrum of ZnO/SnO₂-based PSCs. (d) Nyquist plots of ZnO-based and ZnO/SnO₂-based PSCs.

induced by the ETL with an energy level gradient. As illustrated in Figure 5a, the PL of the ZnO/SnO₂-based perovskite film quenches more efficiently than that of the ZnO nanowire-based perovskite film indicating stronger electron extraction in the ZnO/SnO₂ structure [38]. This result is in good agreement with the TRPL measurements shown in Figure 5b, where the ZnO nanowire-based samples exhibited a much longer lifetime (158.4 ns) than that of the ZnO/SnO₂ structure (102.0 ns). Both curves were fitted with a two-exponential decay algorithm according to previous reports [39,40], and detailed parameters about the TRPL lifetime are shown in Table S2. The EQE spectra of the ZnO/SnO₂-based device shows a higher carrier harvesting than in the ZnO-nanowire-based device along the entire absorption range of 400-800 nm, especially in the long wavelength band in Figure 5c. The integrated photocurrent densities are 21.26 and 22.16 mA/cm², respectively, which are in good agreement with the J_{sc} derived from the $J-V$ measurement. Figure 5d shows the EIS of the PSCs tested with bias voltage. The recombination

PSCs.

To shine further light into the enhanced charge extraction dynamics of the PSCs with an interfacial gradient energy band engineering, transient photocurrent (TPC) delay and photovoltage (TPV) delay were utilized to characterize the charge transport and recombination time constants (τ_t and τ_r , Table S3) [41]. The τ_t decreased from 64 to 34 ns after the ETL with an energy band gradient was introduced (Figure 6a), confirming that the photogenerated charge transport through the ETL with an energy band gradient was faster than that through the sample with the ZnO nanowire ETL. Meanwhile, τ_r values of 0.95 μ s and 1.45 μ s were derived for the ZnO nanowire-based and ZnO/SnO₂-based PSCs, respectively (Figure 6b). The long photovoltage delay time in the ZnO/SnO₂-based PSCs resulted from the slow interfacial photogenerated charge recombination. Therefore, the introduced SnO₂ layer not only enhanced the electron extraction from the perovskite materials but also suppressed the electron accumulation at the interface of the ETL and

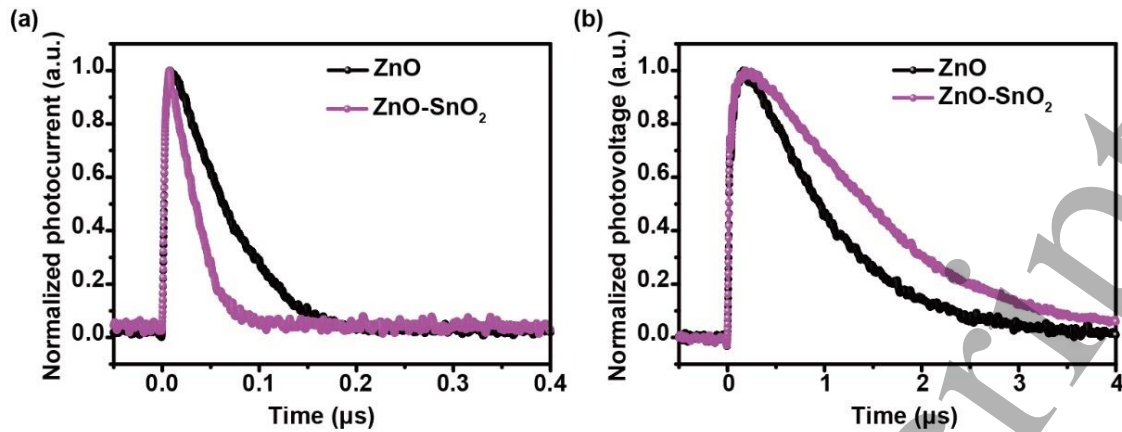


Figure.6 Charge transfer dynamics in devices with different ETLs. (a) Transient photocurrent decay curves of PSCs with ZnO/SnO₂ (purple) and ZnO (black) as ETLs. (b) Transient photovoltage decay curves of PSCs with ZnO/SnO₂ (purple) and ZnO (black) as ETLs.

perovskite materials. By introducing SnO₂ nanocrystal layers as an interfacial engineering, the establishment of an ETL with an energy level gradient and interfacial passivation were the dominant factor responsible for the enhancement of the ZnO nanowire-based PSCs.

3. Conclusion

We demonstrate interfacial engineering by introducing SnO₂ nanocrystal at the interface between ZnO NWs and perovskite materials to enhance electron extraction and restrict surface recombination. A PCE of over 18 % was reached in this study, and the ZnO/SnO₂-based PSCs exhibit good thermal stability at 40 °C for over 500 h. This work offers a general way to improve the performance of ZnO nanowire-based PSCs under low-temperature synthesis, which is favorable for the fabrication of flexible and stretchable perovskite solar cells.

Supporting Information

This supporting information includes Method Section, Figures S1~S6 and Tables S1~S3: fabrication process, cross-section SEM, *J-V* curves scanned by different rates, and photovoltaic parameters of devices.

Acknowledgements

The authors thank the National Natural Science Foundation of China (No. U1704138, 11674290, 51622205, 61675027, 61405040, 51432005, 61505010, 51722201, 51672008, 91733301 and 51502018), the National Key R & D Project from Minister of Science and Technology, China (2016YFA0202703 and 2017YFA0206701), Beijing City Council of Science and Technology (Z171100002017019 and Z181100004418004), Natural Science Foundation of Beijing Municipality (4181004, 4182080, 4184110, 2184131 and Z180011), and Shenzhen Science and Technology Program (Grant No.KQTD20170810105439418).

References

- [1] Cao Y, Wang N, Tian H, Guo J, Wei Y, Chen H, Miao Y, Zou W, Pan K, He Y, Cao H, Ke Y, Xu M, Wang Y, Yang M, Du K, Fu Z, Kong D, Dai D, Jin Y, Li G, Li H, Peng Q, Wang J and Huang W 2018 *Nature* **562** 249-53
- [2] Lin K, Xing J, Quan L N, de Arquer F P G, Gong X, Lu J, Xie L, Zhao W, Zhang D, Yan C, Li W, Liu X, Lu Y, Kirman J, Sargent E H, Xiong Q, and Wei Z 2018 *Nature* **562** 245
- [3] Chiba T, Hayashi Y, Ebe H, Hoshi K, Sato J, Sato S, Pu Y-J, Ohisa S, and Kido J 2018 *Nat. Photon.* **12** 681
- [4] Liu K-K, Liu Q, Yang D-W, Liang Y-C, Sui L-Z, Wei J-Y, Xue G-W, Zhao W-B, Wu X-Y, Dong L, and Shan C-X 2020 *Light: Sci. Appl.* **9** 44
- [5] Xu W, Hu Q, Bai S, Bao C, Miao Y, Yuan Z, Borzda T, Barker A J, Tyukalova E, Hu Z, Kawecki M, Wang H, Yan Z, Liu X, Shi X, Uvdal K, Fahlman M, Zhang W, Duchamp M, Liu J-M, Petrozza A, Wang J, Liu L-M, Huang W, and Gao F 2019 *Nat. Photon.* **13** 418
- [6] Zhu H, Fu Y, Meng F, Wu X, Gong Z, Ding Q, Gustafsson M V, Trinh M T, Jin S, and Zhu X Y 2015 *Nat. Mater.* **14** 636
- [7] Li F, Lu J, Zhang Q, Peng D, Yang Z, Xu Q, Pan C, Pan A, Li T, and Wang R 2019 *Sci. Bull.* **64** 698
- [8] Yang Z, Lu J, ZhuGe M, Cheng Y, Hu J, Li F, Qiao S, Zhang Y, Hu G, Yang Q, Peng D, Liu K, and Pan C 2019 *Adv. Mater.* **31** 1900647
- [9] Lai Q, Zhu L, Pang Y, Xu L, Chen J, Ren Z, Luo J, Wang L, Chen L, Han K, Lin P, Li D, Lin S, Chen B, Pan C, and Wang Z L 2018 *ACS Nano* **12** 10501
- [10] Wu W, Wang X, Han X, Yang Z, Gao G, Zhang Y, Hu J, Tan Y, Pan A, and Pan C 2019 *Adv. Mater.* **31** 1805913
- [11] Yang Z, Xu Q, Wang X, Lu J, Wang H, Li F, Zhang L, Hu G, and Pan C 2018 *Adv. Mater.* **30** 1802110
- [12] Huang Y, Zhang Y, Sun J, Wang X, Sun J, Chen Q, Pan C, and Zhou H 2018 *Adv. Mater. Interfaces* **5** 1800224
- [13] Ding J, Han Q, Ge Q-Q, Xue D-J, Ma J-Y, Zhao B-Y, Chen Y-X, Liu J, Mitzi D B, and Hu J-S 2019 *Joule* **3** 402
- [14] Yao K, Leng S, Liu Z, Fei L, Chen Y, Li S, Zhou N, Zhang J, Xu Y-X, and Zhou L 2019 *Joule* **3** 417

- 1
2
3 [15] Jung E H, Jeon N J, Park E Y, Moon C S, Shin T J, Yang T-Y,
4 Noh J H, and Seo J 2019 *Nature* **567** 511
- 5 [16] Sun J, Hua Q, Zhou R, Li D, Guo W, Li X, Hu G, Shan C, Meng
6 Q, Dong L, Pan C, and Wang Z L 2019 *ACS Nano* **13** 4507
- 7 [17] Wang L, Zhou H, Hu J, Huang B, Sun M, Dong B, Zheng G,
8 Huang Y, Chen Y, and Li L 2019 *Science* **363** 265
- 9 [18] Dong Q, Fang Y, Shao Y, Mulligan P, Qiu J, Cao L, and Huang
10 J 2015 *Science* **347** 967
- 11 [19] Jeon N J, Na H, Jung E H, Yang T-Y, Lee Y G, Kim G, Shin H-
12 W, Seok S I, Lee J, and Seo J 2018 *Nat. Energy* **3** 682
- 13 [20] Hua Q, Sun J, Liu H, Bao R, Yu R, Zhai J, Pan C, and Wang Z
14 L 2018 *Nat. Commun.* **9** 244
- 15 [21] Wang Y, Cheng X, Yuan K, Wan Y, Li P, Deng Y, Yu H, Xu
16 X, Zeng Y, Xu W, Li Y, Ma R, Watanabe K, Taniguchi T, Ye Y,
17 and Dai L 2018 *Sci. Bull.* **63** 1576
- 18 [22] Wang C, Zhao J, Ma C, Sun J, Tian L, Li X, Li F, Han X, Liu
19 C, Shen C, Dong L, Yang J, and Pan C 2017 *Nano Energy* **34** 578
- 20 [23] Pan C, Dong L, Zhu G, Niu S, Yu R, Yang Q, Liu Y, and Wang
21 Z L 2013 *Nat. Photon.* **7** 752
- 22 [24] Zhang J, Tan C H, Du T, Morbidoni M, Lin C-T, Xu S, Durrant
23 J R, and McLachlan M A 2018 *Sci. Bull.* **63** 343
- 24 [25] Lu Y-J, Shi Z-F, Shan C-X, and Shen D-Z 2017 *Chin. Phys. B*
25 **26** 047703
- 26 [26] Qiao S, Liu J, Fu G, Ren K, Li Z, Wang S, and Pan C 2018 *Nano*
27 *Energy* **49** 508
- 28 [27] Pelicano C M and Yanagi H 2019 *Appl. Surf. Sci.* **467-468** 932
- 29 [28] Pelicano C M and Yanagi H 2020 *Appl. Surf. Sci.* **506** 144917
- 30 [29] Li N, Meng F, Huang F, Yu G, Wang Z, Yan J, Zhang Y, Ai
31 Y, Shou C, Zeng Y, Sheng J, Yan B, and Ye J 2020 *ACS Appl.*
32 *Energy Mater.* **3** 9610
- 33 [30] Felizco J, Juntunen T, Uenuma M, Etula J, Tossi C, Ishikawa
34 Y, Tittonen I, and Uraoka Y 2020 *ACS Appl. Mater. Interfaces*
35 **12** 49210
- 36 [31] Zhang P, Wu J, Zhang T, Wang Y, Liu D, Chen H, Ji L, Liu C,
37 Ahmad W, Chen Z D, and Li S 2018 *Adv. Mater.* **30** 1703737
- 38 [32] Li S, Zhang P, Chen H, Wang Y, Liu D, Wu J, Sarvari H, and
39 Chen Z D 2017 *J. Power Sources* **342** 990
- 40 [33] Ralaifarisoa M, Salzmann I, Zu F S, and Koch N 2018 *Adv.*
41 *Electron. Mater.* **4** 1800307
- 42 [34] Li Z, Wang R, Xue J, Xing X, Yu C, Huang T, Chu J, Wang
43 K-L, Dong C, Wei Z, Zhao Y, Wang Z-K, and Yang Y 2019 *J.*
44 *Am. Chem. Soc.* **141** 17610
- 45 [35] Noh Y W, Jin I S, Kim K S, Park S H, and Jung J W 2020 *J.*
46 *Mater. Chem. A* **8** 17163
- 47 [36] Lin L, Yang Z, Jiang E, Wang Z, Yan J, Li N, Wang Z, Ai Y,
48 Shou C, Yan B, Zhu Y, Sheng J, and Ye J 2019 *ACS Appl.*
49 *Energy Mater.* **2** 7062
- 50 [37] Zhao C, Chen B, Qiao X, Luan L, Lu K, and Hu B 2015 *Adv.*
51 *Energy Mater.* **5** 1500279
- 52 [38] Jiang Q, Zhang L, Wang H, Yang X, Meng J, Liu H, Yin Z, Wu
53 J, Zhang X, and You J 2017 *Nat. Energy* **2** 16177
- 54 [39] Zuo L, Gu Z, Ye T, Fu W, Wu G, Li H, and Chen H 2015 *J. Am.*
55 *Chem. Soc.* **137** 2674
- 56 [40] Chen Q, Zhou H, Song T-B, Luo S, Hong Z, Duan H-S, Dou L,
57 Liu Y, and Yang Y 2014 *Nano Lett.* **14** 4158
- 58 [41] Chen W, Wu Y, Yue Y, Liu J, Zhang W, Yang X, Chen H, Bi
59 E, Ashrafali I, and Grätzel M 2015 *Science* **350** 944
- 60